Jour. Korean Inst. Mining Geol.
Vol. 25, No. 2, p. 115-131, 1992.

Cretaceous Epithermal Au-Ag Mineralization in the Muju-Yeongam District (Sulcheon Mineralized Area), Republic of Korea

Chil-Sup So*, Seong-Taek Yun, Sang-Hoon Choi*, Se-Hyun Kim*** and Moon-Young Kim******

ABSTRACT : Late Cretaceous (90.5 Ma), epithermal gold-silver·vein mineralization of the Weolseong and Samchang mines in the Sulcheon area, 60 km southeast of Taejeon, can be separated into two distinct stages (I and II) during which fault-related fissures in Precambrian gneiss and Cretaceous (102 Ma) porphyritic granite were filled. Fluid inclusion and mineralogical data suggest that quartz-sulfide-electrum-argentite-forming stage I evolved from initial high temperatures (≈ 340°C) to later lower temperatures (≈ 140°C) at shallow depths of about 400 to 700 m. Ore fluid salinities were in the range between 0.2 and 6.6 wt. % eq. NaCl. A simple statistic model for fluid-fluid mixing indicates that the mixing ratio (the volumetric ratio between deep hydrothermal fluids and meteoric water) systematically decreased with time. Gold-silver deposition occurred at temperatures of 230± 40°C mainly as a result of progressive cooling of ore-forming fluids through mixing with less-evolved meteoric waters.

Measured and calculated hydrogen and oxygen isotope values of hydrothermal fluids indicate meteoric water dominance, approaching unexchanged meteoric water values. The geologic, mineralogic, and geochemical data from the Weolseong and Samchang mines are similar to those from other Korean epithermal gold-silver vein deposits.

INTRODUCTION

Gold-silver vein deposits in South Korea are fissure-filling quartz± carbonate veins intimately associated with Jurassic and Cretaceous granites (Shimazaki et al., 1981, 1986). Three main types of deposit have been documented, based on mineralization age, Au/Ag ratio, depth of formation, water-rock ratio (Shelton et al., 1988). These are: gold-rich mesothermal gold deposits, Korean-type gold-silver deposits, and more silver-rich epithermal deposits.

Within the Sulcheon area, there are many gold-silver deposits made the area one of the largest and most productive gold-silver mine districts in South Korea (Kim, 1971). The Weolseong and Samchang mines are examples of the numerous gold-silver deposits in the Sulcheon area. Ore grades of the Weolseong mine were reported to be 5.2 to 18.5 g/ton Au and 48 to 73 g/ton Ag. Ore reserves are not known.

Studies of the Weolseong and Samchang mines were undertaken in order to understand the physicochemical conditions and origin of the ore fluids in the Sulcheon area. Data of the present study are compared with those from other epithermal gold-silver deposits in Korea.

* Department of Geology, Korea University, Seoul, Republic of Korea (고려대학교 지질학과)
** Department of Mineral and Energy Resources Engineering, Semyung University, Jecheon 390-230, Republic of Korea (세명대학교 자원공학과)
*** Department of Mineral Resources, Sangji University, Weonju, Republic of Korea (상지대학교 자원공학과)
**** Korea Institute of Energy and Resources, Taejeon 152-600, Republic of Korea (한국동력자원연구소 비금속실)

GEOLOGIC SETTING

The Sulcheon Au-Ag mine area is located approximately 60 km southeast of Taejeon within the Sobaegsan Massif. The massif forms the basement of southern parts of Korean peninsula, and is mainly composed of Precambrian metamorphic rocks.

Rocks in the mine area, from oldest to youngest units, is composed of Precambrian gneiss complex, age-unknown amphibolite, and Cretaceous porphyritic granite and felsic dykes (Fig. 1).

The Precambrian gneiss complex occupies most of the mine area, and consists of migmatitic gneiss,

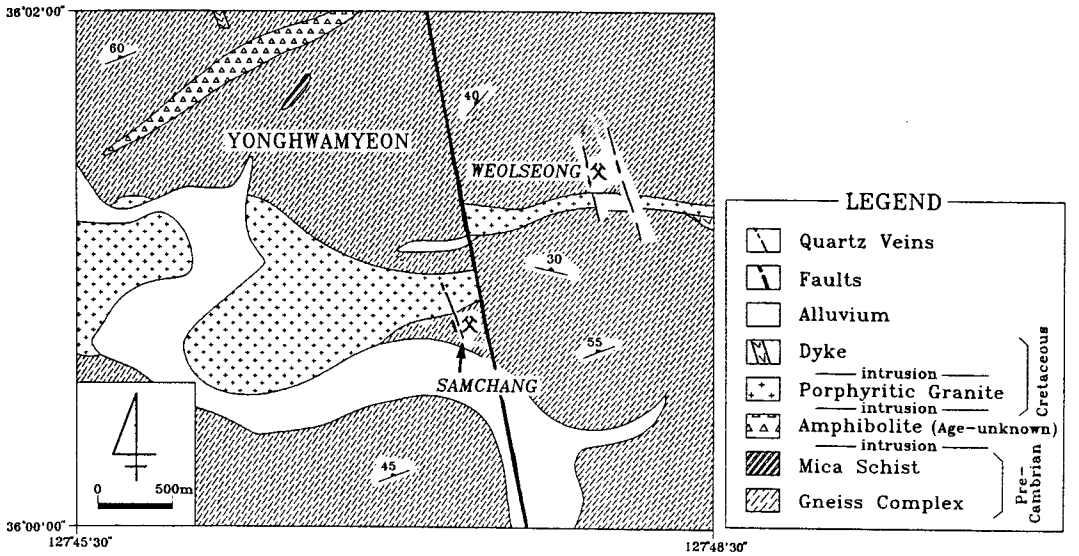

Fig. 1. Geologic map of the Weolseong and Samchang Au-Ag mine area.

biotite banded gneiss, granitic gneiss and mica schist. The biotite banded gneiss is locally severely migmatized and injected with remobilized granitic material. Mica schist occurs as small intercalations generally parallel to the schistosity of surrounding gneisses. The orientation of the schistosity is variable, but mainly strikes N15°~45°E and dips 50°~80°SE. Choo and Kim (1985) obtained a whole-rock Rb-Sr isochron of 1,810± 10 Ma for the granitic gneiss in the Kimcheon-Sangju area. They found that some data, especially from the migmatitic samples, plotted away from the isochron, forming clusters of 1,608, 402, and 172 Ma. Lee (1986) suggested that the metamorphic rocks in the southwest of the Sobaegsan Massif originated from shales and graywackes subjected to polymetamorphism ranging from upper amphibolite facies to epidote-amphibolite facies with locallized greenschist facies. Amphibolite occurs as NE-trending lensoid bodies that discordantly intrude the gneiss complex. It is composed mainly of hornblende and plagioclase with minor amounts of biotite, quartz and chlorite.

The porphyritic granite intrudes all the rocks described above in the mine area. It is typically medium-grained and porphyritic, but its margins are fine-grained and more biotite-rich. The eastern part of the granite assumes a narrow (<30 m wide) dyke-like shape (Fig. 1) whose lithology is more close to granite porphyry than to granite. The granite yielded a Rb-Sr isochron of 102± 9 Ma (So and Yun, in prep.). Youn and Park (1991) reported a biotite K-Ar age of 98.7± 3.6 Ma. Detailed lithochemical characteristics of the granite are described in Youn and Park (1991).

An N15°W-trending fault and related tensional fractures cut all the rock units in the mine area (Fig. 1). Au-Ag-bearing quartz veins and ubiquitous felsic dykes occupy these fault-related tension fractures in Cretaceous porphyritic granite and in the nearby Precambrian gneiss. This relationship suggests that the NW-trending fault acted as a major conduit for gold-silver-mineralizing fluids.

ORE VEIN AND HYDROTHERMAL ALTERATION

The Weolseong mine consists of four veins which generally strike N10°~25°W, dip 75°~85°SW, and extend horizontally for <500 m along strike with an average vein thickness of about 0.3 m. The Samchang mine consists of two subparallel veins which strike N15°~20°W, and dip 75°~80°SW. The Main vein of the Samchang mine can be traced horizontally for over 300 m. Its thickness varies from 0.2~1.0 m.

Mineralized veins of the Weolseong and Samchang mines consist of a single generation of white quartz with pyrite, base-metal sulfides, electrum and argentite. The quartz veins exhibit several textural varieties such as crustification, brecciation, and open vugs. White calcite veins with rare pyrite fill irregular fractures in the quartz veins.

Hydrothermal wall-rock alteration zones occur in gneiss and granite, bleaching the rocks green or

white. Chloritization and pyritization of host gneiss (especially the biotite banded gneiss) extends up to 0.2 m from vein margins. Porphyritic biotite granite has distinct alteration zones (usually up to 0.5 m wide). The alteration, from inner to outer zones, is as follows: silicic, sericitic, and chloritic. The sericitic alteration zones are characterized by obliteration of feldspar and biotite. Sericite locally comprises up to 75 volume percent of the altered rock. Minor illite occurs in the innermost zones of sericitic alteration. Fine-grained euhedral pyrite is common within the sericitized zones. The chloritic zones are characterized by alteration of biotite to chlorite plus pyrite, and by feldspar phenocrysts that appear to be dusty due to development of microscopic-sized sericites.

An alteration sericite yielded a K-Ar date of 90.5± 1.1 Ma (So and Yun, in prep.), suggesting a Late Cretaceous age of gold-silver mineralization. The mineralization may be associated with ubiquitous felsic dykes in the mine area, rather than with the older porphyritic biotite granite.

VEIN MINERALOGY

Vein minerals of the Weolseong and Samchang Au-Ag deposits were deposited in two distinct mineralization stages (I and II) which were separated by a tectonic fracturing event (Fig. 2). Stage I was quartz-sulfide-electrum-argentite mineralization. Stage II was post-ore carbonate mineralization stage which filled newly opened fractures.

Stage I

Economic quantities of gold and silver, together with quartz and sulfides were deposited during this stage. The principal sulfides of stage I were pyrite, sphalerite and galena, and the minor sulfides were chalcopyrite, arsenopyrite and pyrrhotite. Stage I mineralization can be further divided into three substages, based on mineral assemblages and textural relationships: (1) Early substage (pyrite, arsenopyrite and dark sphalerite); (2) Middle substage (sphalerite, galena, electrum and argentite); and (3) Late (Vug) substage (pyrite and calcite).

Early Substage

The Early Substage is characterized by massive milky to gray quartz associated with pyrite and dark sphalerite. Minerals of this substage occur as follows: 1) thin veins and stockworks within sericitized rocks; 2) discontinuous segments near vein margins; and

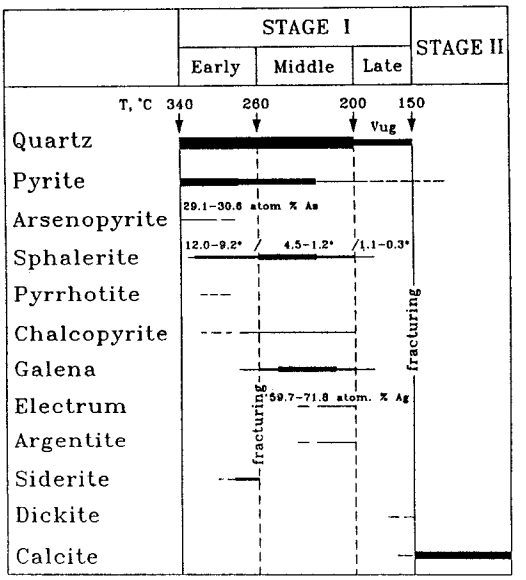

Fig. 2. Generalized paragenetic sequence of vein minerals from the Weolseong and Samchang Au-Ag mines. Line widths indicate relative abundance. Temperature scale (T, °C) is based on fluid inclusion homogenization temperatures. *; mole % FeS of sphalerite.

3) fragments enclosed within later white quartz veins. The quartz locally occurs as gray chalcedonic bands near vein margins.

Early-Substage pyrite, the major sulfide, occurs as ubiquitous, fine to coarse crystalline aggregates within quartz veins and altered wall-rocks. Earliest fine-grained pyrite commonly forms massive bands near vein margins, and includes euhedral to subhedral arsenopyrite that contains 29.1 to 30.6 atom. % As (Table 1). Rare pyrrhotite occurs as tiny inclusions within pyrite and dark sphalerite.

Early-Substage sphalerite is typically black and closely intergrown with pyrite. It commonly includes blebs of chalcopyrite and rare pyrrhotite. The sphalerite is characteristically iron-rich, with mole % FeS ranging from 9.2 to 12.0 % (Table 1 and Fig. 3). Siderite occurs locally intergrown with sphalerite in thin veins cutting the altered granites.

Early-Substage sulfides, especially pyrite and sphalerite are often brecciated and cemented by the Middle-Substage minerals. This indicates that a fracturing event occurred after the Early-Substage mineralization.

Middle Substage

The Middle Substage is characterized by white comb quartz associated with yellow-brown sphalerite

Table 1. Chemical compositions of arsenopyrite, sphalerite, and electrum from the Weolseong and Samchang Au-Ag mines.

A. arsenopyrite

Mine	Sample no.	Substage	Associated minerals	wt. %				atom. %		
				Fe	As	S	total	Fe	As	S
Weolseong	WS-2-3	Early	py, sp	34.62	41.87	23.72	100.21	32.31	29.13	38.56
				35.26	42.47	22.73	100.46	33.10	29.72	37.17
				34.76	42.39	23.21	100.36	32.55	29.59	37.86
	WS-3-2	Early	py, sp, po	35.08	42.38	22.07	99.53	33.37	30.05	36.57
				33.84	43.22	23.36	100.42	31.70	30.18	38.12
				34.79	42.78	22.08	99.64	33.09	30.33	36.58
Samchang	SC-15	Early	py	34.48	42.14	22.08	98.69	33.05	30.10	36.85
	SC-17	Early	py, sp	34.98	41.95	21.92	98.85	33.49	29.94	36.56
				35.27	42.83	22.02	100.12	33.41	30.25	36.33
				34.49	43.56	22.42	100.47	32.53	30.63	36.84

B. Sphalerite

Mine	Sample no.	Substage	Associated minerals	wt. %			atom. %		
				Fe	Mn	Cd	FeS	MnS	CdS
Weolseong	WS-1-3	Early	py, apy	7.16	0.16	0.18	12.01	0.30	0.23
	WS-2-1	Late	py, gn	0.65	0.08	0.40	1.10	0.12	0.52
				0.54	0.02	0.34	0.90	0.03	0.44
				0.51	0.00	0.42	0.85	0.00	0.54
	WS-2-2	Early	py, apy	5.49	0.05	0.14	9.21	0.10	0.19
				6.61	0.06	0.09	11.09	0.10	0.11
	WS-4-2	Middle	py, gn, el, arg	1.80	0.02	0.29	3.02	0.04	0.39
				1.74	0.03	0.23	2.92	0.05	0.30
	WS-7-1	Middle	py, gn, cp	1.17	0.00	0.42	1.97	0.00	0.54
	WS-7-3	Middle	py, gn	2.70	0.00	0.41	4.53	0.00	0.53
				2.45	0.03	0.16	4.14	0.06	0.21
				0.88	0.03	0.33	1.47	0.05	0.42
Samchang	SC-5-1	Middle	py, gn	0.91	0.02	0.17	1.53	0.03	0.22
				0.93	0.02	0.24	1.56	0.03	0.31
	SC-10-2	Middle	py, gn	0.82	0.34	0.21	1.38	0.07	0.27
				0.83	0.02	0.38	1.40	0.04	0.49
				0.72	0.02	0.19	1.21	0.03	0.25
	SC-12-1	Late	py	0.50	0.11	0.34	0.84	0.21	0.45
				0.19	0.01	0.19	0.32	0.02	0.24

C. Electrum

Mine	Sample no.	Substage	Associated minerals	wt. %			atom. %	
				Au	Ag	total	Au	Ag
Weolseong	WS-4-2	Middle	py, sp, gn, arg	55.05	44.70	99.75	40.28	59.72
				53.45	49.96	100.41	33.12	66.88
				50.42	47.85	98.27	31.71	68.29
				46.27	53.58	99.85	28.24	71.76

Abbreviation: apy=arsenopyrite, arg=argentite, cp=chalocopyrite, el=electrum, gn=galena, po=pyrrhotite, py=pyrite, sp=sphalerite

and galena. The yellow-brown sphalerite (1.2 to 4.5 mole % FeS; Table 1 and Fig. 3) commonly occuras anhedral aggregates near vein margins, which are closely associated with pyrite, galena and chal-

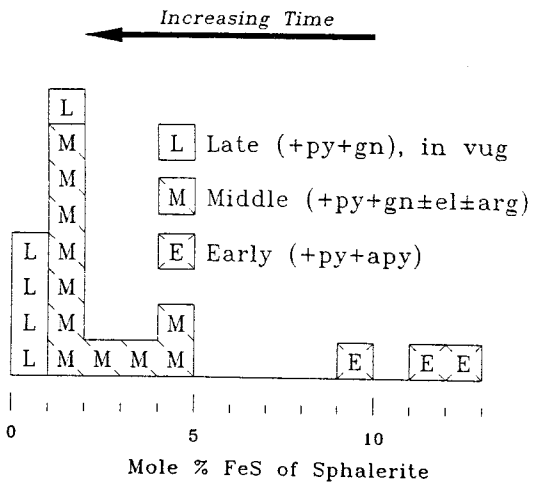

Fig. 3. Variation of iron content (mole % FeS) of sphalerite from the Weolseong and Samchang Au-Ag mines. Abbreviations: apy=arsenopyrite, arg=argentite, el=electrum. gn=galena, py=pyrite.

copyrite. Microscopic chalcopyrite veinlets crosscut the Early-Substage sphalerite and pyrite.

Electrum occurs as fine irregular grains occupying fractures in Early-Substage pyrites. It is intergrown with galena, sphalerite (≈ 3 mole % FeS) and argentite. Silver contents (atom. % Ag) of electrum grains are 59.7 to 71.8% by EPMA (Table 1).

Late (Vug) Substage

Pyrite, sphalerite, galena, dickite and calcite were deposited in vugs during the close of stage I. Fine-grained, honey-colored sphalerite (0.3 to 1.1 mole % FeS; Table 1 and Fig. 3) and galena are rarely intergrown with vug quartz. Fine (<1 mm) pyrite cubes, white dickite powders, and white calcite rhombs rarely coat and overgrow vug quartz, although they do not coexist together at a single locality.

Stage II

Following stage I mineralization, tectonic activity resulted in extensive brecciation and fracturing of stage I veins. The newly opened fractures (<10 cm wide) were filled with barren, white calcite with rare pyrite.

FLUID INCLUSION STUDIES

701 fluid inclusion (450 primary and 251 secondary) in 33 samples of quartz, sphalerite, and calcite were examined in order to document composition and temperature ranges of hydrothermal fluids during the mineralization at the Weolseong and Samchang mines.

Microthermometric data were obtained on a Fluid Inc. gas-flow heating/freezing system. Temperatures of total homogenization and final ice melting have standard errors of ± 1.0° and ± 0.2°C, respectively. Salinity data are reported based on freezing-point depressions in the system H_2O-NaCl (Potter et al., 1978).

Two types of fluid inclusion were observed: liquid-rich (type I), and vapor-rich (type II) fluid inclusions. Liquid-rich inclusions are the predominant type and contain a liquid and a vapor bubble comprising <10 to 35 vol. percent at 25°C. The bubbles were determined (by crushing) to be essentially water vapor. No traces of gas hydrates were observed during freezing. Initial (eutectic) melting of ice was measured for some liquid-rich inclusions, and occurred at ≈ −20°C. This indicates that NaCl was the dominant dissolved salt (cf. Crawford, 1981).

Vapor-rich inclusions contain a liquid and a vapor bubble comprising >60 vol. percent at 25°C. They occur only as primary inclusions in milky to gray quartz of the Early stage I, and homogenize to the vapor phase.

All samples examined contained both primary and secondary fluid inclusions. Most samples had a higher proportion of secondary inclusions, probably due to repeated fracturing and healing both during and after quartz deposition. Obvious secondary inclusions occur along healed fractures and have small (<15 vol. %) vapor proportions. However, it was often difficult to distinguish between true primary and secondary inclusions using normal criteria (Roedder, 1984) because many secondary inclusions appeared to be primary-like inclusions as reported by Sterner and Bodnar (1984). Therefore, we have taken special care in selecting adequate samples for our fluid inclusion study, and in distinguishment between primary and secondary inclusions.

Microthermometric Data

Microthermometric data of fluid inclusions are summarized in Table 2 and Figs. 4 and 5. Inclusions in each type of mineral from the Weolseong and Samchang mines have similar ranges of homogenization temperature and salinity (Figs. 4 and 5).

Primary fluid inclusions in stage I minerals were homogenized at wide temperatures between 138° and 338°C (Fig. 4). This wide temperature range is

Table 2. Summary of microthermometric data of fluid inclusions from the Weolseong and Samchang Au-Ag mines.

Mine	Stage	Substage	Mineral	Inclusion type	T_h(°C) Range	T_h(°C) Average[1)]	Salinity (wt. % eq. NaCl) Range	Salinity (wt. % eq. NaCl) Average[1)]
Weolseong	I	Early	milk to gr qtz	PI	237~338	282(81)	2.7~6.6	4.8(31)
				PII	283~316	299(6)	5.2~5.7	5.4(3)
				SI	157~242	189(62)	0.9~4.8	3.3(25)
		Middle	wht qtz	PI	192~271	232(74)	2.2~6.6	3.9(31)
				SI	144~198	182(53)	0.9~3.6	2.3(21)
			sp	PI	214~241	229(7)	4.8~5.8	5.2(4)
				SI	159~197	180(16)	1.7~3.2	2.5(6)
		Late(Vug)	cl qtz	PI	146~213	184(65)	0.2~4.6	2.7(32)
	II	–	cc	PI	138~177	157(26)	0.4~3.1	2.0(13)
Samchang	I	Early	milk to gr qtz	PI	246~322	289(68)	3.4~6.3	4.7(24)
				PII	282~293	288(4)	5.8	5.8(1)
				SI	164~244	193(73)	1.2~4.0	2.9(14)
		Middle	wht qtz	PI	202~261	233(58)	1.4~6.1	3.2(23)
				SI	158~207	185(47)	1.0~3.7	2.2(14)
		Late(Vug)	cl qtz	PI	138~211	185(61)	0.7~4.8	2.3(25)

[1)] Numbers in parentheses refer to number of inclusions measured. Abbreviation: I=liquid-rich inclusions, II=vapor-rich inclusions, cc=calcite, cl=clear, gr=gray, milk=milky, P=primary, qtz=quartz, S=secondary, sp=sphalerite, wht=white.

thought to reflect a continuum of several episodes of hydrothermal activity rather than one specific event. Specific temperature ranges for each substage are: Early Substage, 237° to 338°C; Middle Substage, 192° to 271°C; and Late (Vug) Substage, 138° to 213 °C. Vapor-rich (type II) inclusions in milky to gray quartz (Early substage) were homogenized to vapor at temperatures of 282° to 316°C.

Salinities of primary inclusions in stage I minerals range from 0.2 to 6.6 wt. % eq. NaCl (Fig. 5). Within each substage the values are: Early Substage, 2.7 to 6.6 wt. % (for vapor-rich inclusions, 5.2~5.8 %); Middle Substage, 1.4 to 6.6 wt %; and Late (Vug) Substage, 0.2 to 4.8 wt. %.

Primary liquid-rich inclusions in stage II calcite have homogenization temperatures of 138° to 177°C and salinities of 0.4 to 3.1 wt. % eq. NaCl.

Within Stage I mineralization, the temperatures and salinities of each substage's primary fluid inclusions are nearly identical to those of secondary, low-temperature fluid inclusions in former substages (see peaks in histograms of secondary inclusions in Figs. 4 and 5). Shelton and Orville (1980) showed that secondary fluid inclusions can be trapped along healed fractures in quartz within hours under geologically reasonable conditions. Fractures were present throughout Stage I mineralization in the Weolseong and Samchang mines. Therefore, it is likely that primary fluids during the Middle and Late substages were trapped as secondary inclusions in minerals of previous substages. This may indicate that the fluids of the later substages passed rather pervasively through earlier-formed vein systems.

Variations in Temperature and Salinity of Hydrothermal Fluids

Fluid inclusion data indicate that stage I evolved from initial high temperatures (≈ 340°C) to lower temperatures (≈ 140°C). It is noteworthy that homogenization temperatures of primary fluid inclusions display a systematic decrease with increasing paragenetic time (through successive substages) (Fig. 4). This indicates that each substage was a distinct mineralizing system which largely abated prior to the onset of the next, and that stage I mineralization progressively cooled with time. Such progressive cooling of stage I fluids was probably a result of progressive introduction of cooler meteoric waters (see below). Temperature data for stage II calcite-depositing fluids indicate continued cooling of fluids by interaction with less evolved meteoric waters (≈ 140°C) (Fig. 4).

Salinity data of hydrothermal fluids show a gradual decrease with increasing time from ≈ 6.5 to ≈ 0 wt. % eq. NaCl (Fig. 5). This indicates a gradual dilution of the fluids, probably also due to the increasing influx of dilute (≈ 0 wt. % eq. NaCl) meteoric waters. Stage II hydrothermal fluids that deposited calcite must have been much diluted (Fig. 5).

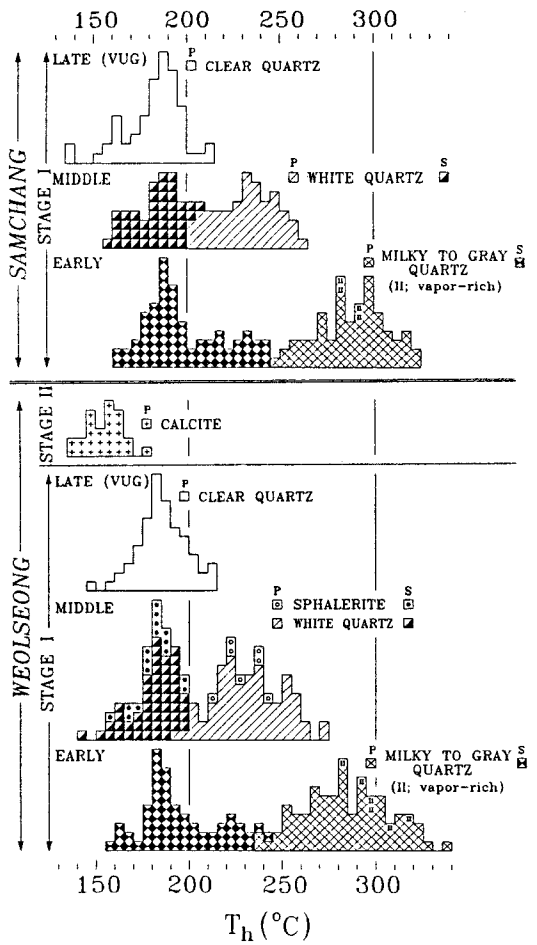

Fig. 4. Histograms of homogenization temperatures of fluid inclusions in vein minerals from the Weolseong and Samchang Au-Ag mines. P=primary inclusions, S= secondary inclusions.

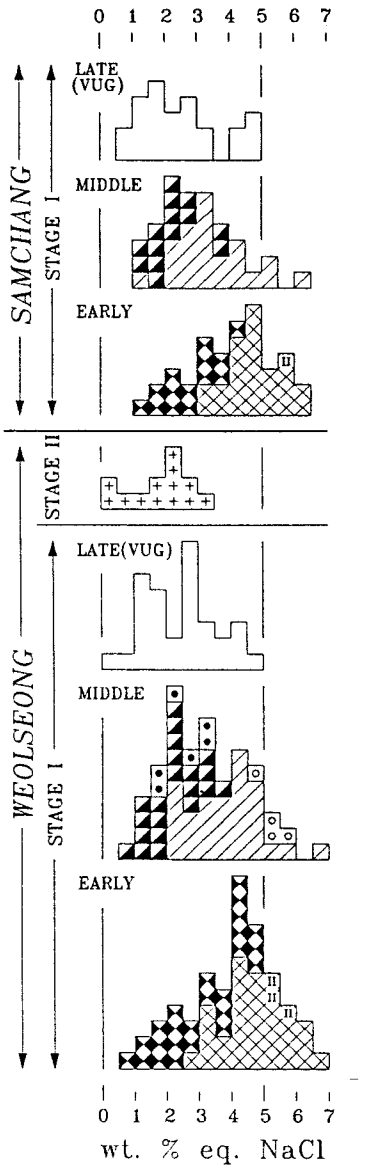

Fig. 5. Histograms of salinities of fluid inclusions in vein minerals from the Weolseong and Samchang Au-Ag mines. Symbols are the same as in Fig. 4.

Measured salinities of some vapor-rich (type II) fluid inclusions in the Early-Substage quartz (≈5~8 wt. % NaCl) are generally higher than those of liquid-rich (type I) inclusions (Fig. 5). The increase in salinity may reflect liquid loss as vapor during boiling (Hedenquist and Henley, 1985).

As described in "VEIN MINERALOGY", Au-Ag minerals (electrum and argentite) were formed only during the Middle Substage of stage I. Homogenization temperatures of primary fluid inclusions in Middle-Substage minerals ranged from 192° to 271°C (Fig. 4), so this temperature range (230° ±40°C)corresponds to the period of Au-Ag ore mineralization. Temperature data from sphalerite (230° ±15°C, Fig. 4) may further constrain the temperature conditions of Au-Ag-depositing fluids because the precious-metal minerals are commonly associated with sphalerite (in adddition to galena).

The relatively narrow range of salinities (most, 2~6 wt. % eq. NaCl) and paucity of vapor-rich fluid inclusions in the Middle-Substage minerals suggest that Au-Ag deposition probably resulted from cooling of the ore fluids. If gold and silver were present as $Au(HS)_2^-$ and $AgCl_2^-$ in solution, then a temperature

Table 3. Volumetric mixing ratios between deep hydrothermal fluids and less-evolved meteoric water, calculated from microthermometric data of primary fluid inclusions from the Weolseong and Samchang Au-Ag mines.

Stage	Substage	T_h(°C)		Salinity(wt. % eq. NaCl)		Mixing ratio	
		Range	Average	Range	Average	From T_h(°C)	From salinity
I	Early	237~338	286	2.7~6.6	4.81	0.49~1.00(0.73)	0.39~1.00(0.72)
	Middle	192~271	232	1.4~6.6	3.71	0.26~0.66(0.46)	0.19~1.00(0.55)
	Late(vug)	138~213	184	0.2~4.8	2.52	0.00~0.37(0.22)	0.00~0.72(0.36)
II	–	138~177	157	0.4~3.1	2.04	0.00~0.19(0.09)	0.03~0.45(0.29)

* The equations used are: $T_{h2}=X \cdot (T_{h1})+(1\text{-}X) \cdot (T_{mw})$, and $S_2=X \cdot (S_1)+(1-X) \cdot (S_{mw})$, where X=mixing ratio (volume of deep hydrothermal fluid), 1−X=volume of introduced less-evolved meteroric water, T_{mw}=temperature (°C) of introduced less-evolved meteoric water, T_{h1}=temperature of deep hydrothermal fluid, T_{h2}=temperature of measured fluid inclusions, S_{mw}=salinity (wt. % eq. NaCl) of introduced less-evolved meteoric water, S_1=salinity of deep hydrothremal fluid, and S_2=salinity introduced less-evolved meteoric water.

* Temperature and salinity of end members of the mixing are chosen as follows, based on measured fluid inclusion data: deep hydrothermal fluid, 340°C and 6.6 wt. % eq. NaCl; and introduced less-evolved meteoric water, 140°C and 0.2 wt. % eq. NaCl.

decrease below 250°C would greatly reduce their solubilities, triggering Au-Ag ore deposition (Seward, 1976, 1984).

Statistic Estimation of Mixing with Less-Evolved Meteoric Water

Homogenization temperatures and salinities of primary and secondary fluid inclusions form the same populations in each substage both from the two mines studied (Table 2, Figs. 4 and 5). This may be estimated by the Mann-Whitney U (Mann and Whitney, 1947) and Kolmogorov-Smirnov (Siegel, 1956) non-parametric tests. Differences in data population may arise when cold, ambient meteoric water enters the interior of the hot mineralizing system.

The progressive decrease in homogenization temperature of primary fluid inclusions with increasing paragenetic time is not best explained by simple conductive cooling of hydrothermal fluids, because the temperature drop observed between each substage is quite large. Heat loss through fluid boiling is not an explanation, because the boiling was observed in only Early-Substage quartz. We prefer the interpretation of progressive inundation of cooler meteoric waters as an effective mechanism of fluid cooling. This is further supported by the gradual decrease in salinity (dilution) of hydrothermal fluids.

Toward the later portions of mineralization, such mixing with less-evolved, cooler meteoric waters became more pronounced, probably due to further fracturing which allowed meteoric waters into the system (see "VEIN MINERALOGY").

Here, we evaluate the mixing model statistically (Table 3), assuming that deep hydrothermal fluids (340°C, 6.6 wt. % eq. NaCl) simply mixed with less-evolved, ambient meteoric waters (140°C, 0.2 wt. % eq. NaCl). Temperature and salinity of the end members of 'parent' fluids which mixed together are inferred from the ranges of fluid inclusion data. The equations used for the calculation are described in Table 3. They indicate that the mixing ratio (volumetric ratio between deep hydrothermal fluids and less-evolved meteoric waters) progressively decreased with increasing time, from 0.73 (for Early Stage I) through 0.46 (for Middle Stage I) and 0.22 (for Late Stage I) to 0.09 (for Stage II) (Table 3). A similar trend of decreasing mixing ratio (from 0.72 to 0.29, Table 3) was obtained using the salinity data. However, this calculation method will have large errors because the salinity data have relatively narrow ranges as well as large errors of measurement.

The above calculation should only be considered as a simple approach to understand the paleohydrology of a hydrothermal system, because hydrothermal fluids for different periods of mineralization would have had and variable initial T-X conditions. However, it indicates a general progressive increase in involvement of less-evolved meteoric-water, and also progressive waning of deep hydrothermal fluid flow due to replacement by local meteoric waters in the mineralizing system.

Pressure-Depth Consideration

Liquid-rich and vapor-rich fluid inclusions are intimately associated in some samples of Early stage

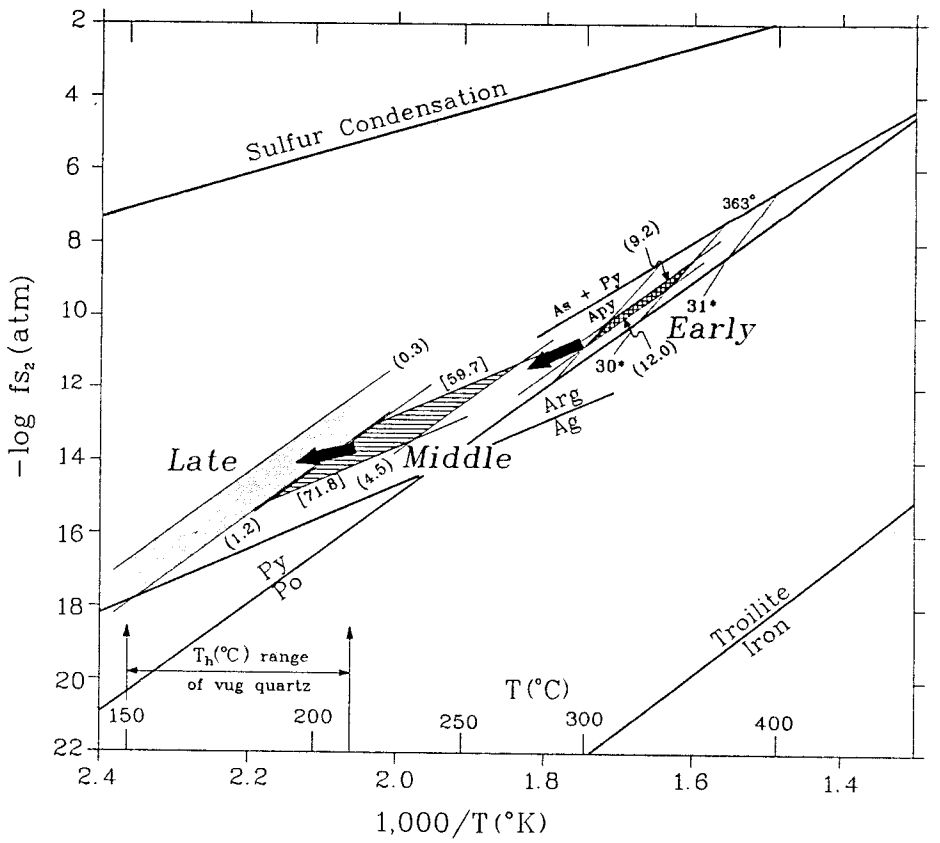

Fig. 6. Fugacity of sulfur versus temperature diagram showing sulifidation reactions pertinent to mineral assemblages of the Weolseong and Samchang Au-Ag mines. Cross-hatched, single hatched, and dotted areas indicate depositional environments of Early, Middle, and Late substages, respectively. Numbers denoted by * are atomic % of As in arsenopyrite. Numbers in [ ] and ( ) are the atomic % of Ag in electrum and the mole % of FeS in sphalerite, respectively. Abbreviations: Ag=native silver, Apy=arsenopyrite, Arg=argentite, As=arsenic, Po=pyrrhotite, Py=pyrite, Th(°C)=homogenization temperature.

I quartz, and tend to homogenize at similar temperatures (282° to 316°C). This phenomenon indicates that fluids boiled during the Early Substage of stage I. The P-T-X data of Sourirajan and Kennedy (1962) and Haas (1971) for the system H_2O-NaCl (5.2 to 5.8 wt. %) indicate pressures of ≈65 to 100 bars for the Early stage I mineralization. These pressures correspond to depths around 720 to 1,200 m assuming lithostatic conditions, and to depths around 230 to 380 m assuming lithostatic conditions. Therefore we suggest that the mineralization occurred at depths of about 400 to 700 m under pressure conditions that fluctuated between lithostatic and hydrostatic.

CHEMISTRY OF ORE FLUIDS

Equilibrium thermodynamic calculations were attempted to estimate the chemical evolution of stage I ore fluids.

Ranges of temperature and fugacity of sulful (fs_2) for stage I fluids were estimated from the phase relations and mineral compositions in the systems Fe-Zn-S (Barton and Toulmin, 1966), Au-Ag-S (Barton and Toulmin, 1964), and Fe-As-S (Kretschmar and Scott, 1976). Figure 6 indicates a general decrease in fs_2 and temperature with time during stage I. Pyrite-arsenopyrite (29.1 to 30.6 atom. % As) -sphalerite (9.2 to 12.0 mole % FeS) assemblages in the Early Substage precipitated within a temperature range of 300° to 350°C, which corresponds to log fs_2 values of −10.9 to −8.4 (Fig. 6). Middle Substage minerals include electrum (59.7 to 71.8 atom % Ag) and more iron-poor sphalerite (1.2 to 4.5 mole % FeS), indicating lower temperature (190° to 275°C) and log fs_2 (−15.1 to −11.3)

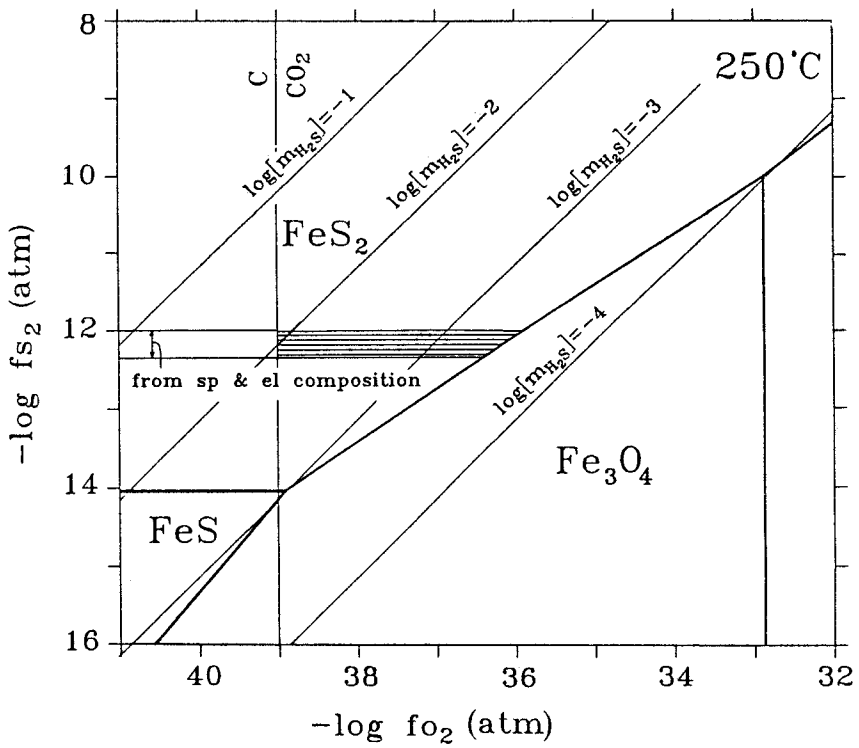

Fig. 7. Fugacity of sulfur versus fugacity of oxygen diagram at 250°C showing mineral stabilities of Middle substage (hatched area). Thick solid lines indicate stability fields of minerals in the system Fe-O-S; vertical thin solid, graphite stability at a log f_{CO_2} of 0.5; oblique thin solid lines, molality of H_2S. Equilibrium constants used for constraining reactions are from Helgeson (1969) and Robie et al. (1978). Abbreviations: el=electrum, sp=sphalerite.

conditions than during the Early Substage. Pyrite and most iron-poor sphalerite (0.3 to 1.1 mole % FeS) were deposited during the Late Substage. Probable log f_{S_2} values for the Late Substage are in the range of −18.0 to −12.3, at a temperature range of 150° to 210°C (based on homogenization temperatures of fluid inclusions in vug quartz). The temperature ranges determined for each substage are in good agreement with the homogenization temperatures of fluid inclusions in vein minerals from each substage (see "FLUID INCLUSION STUDIES").

It is possible to define limits of the fugacities of O_2 and H_2S of the gold-deposited fluid in the Middle Substage using an f_{S_2}-f_{O_2} diagram (Fig. 7). The log f_{S_2} values defined by the compositional isopleths of sphalerite and electrum were −12.0 to −12.3 at 250 °C (Fig. 6). From Fig. 7, the maximum f_{O_2} value is defined by the pyrite-magnetite reaction curve because magnetite is absent. The lower f_{O_2} value is limited by the graphite-CO_2 reaction curve because graphite is absent. The graphite-CO_2 reaction curve is set at a log f_{CO_2} of 0.5 (a maximum value calculated using Henry's law constant for a 0.5 m NaCl solution at 250°C; Ellis and Golding, 1963). For the calculation of log f_{CO_2} value, X_{CO_2} in the gold-depositing fluids was assumed to be lsee than 0.0005, based on the absence of liquid CO_2 and CO_2 hydrates in fluid inclusions. The range of log f_{O_2} for the Middle Substage is about −36 to −39. Under these conditions of low f_{O_2} and f_{S_2}, log molality of H_2S in the ore fluid is in the range of about −2.0 to −3.5 (Fig. 7).

STABLE ISOTOPE STUDIES

In this study we measured th sulfur isotope compositions of 13 samples of vein sulfide, the carbon isotope composition of 1 vein calcite sample, the oxygen isotope compositions of 3 granite whole-rocks samples, 3 samples of vein quartz, and 1 sample of vein calcite, and the hydrogen isotope compositions of 3 inclusion waters from vein quartz. Standard techniques for extraction and analysis were used as described by McCrea (1950), Grinenko (1962), Taylor

Table 4. Sulfur isotope data of stage I sulfides from the Weolseong and Samchang Au-Ag mines.

Mine	Sample no.	Substage	Mineral	$\delta^{34}S$(‰)	$\Delta^{34}S$(‰)[1]	T(°C)[2]	$\delta^{34}S_{H_2S}$(‰)[3]
Weolseong	WS-2-1	Late	pyrite	2.1		200	0.3
	WS-2-2	Early	pyrite	0.3		300	−0.9
	WS-2-3	Early	pyrite	1.9	py-sp	340	0.8
			Sphalerite	1.1	0.8(342± 78)	340	0.8
	WS-2-4	Late	pyrite	1.4		185	−0.5
	WS-4-3	Middle	sphalerite	−1.6	sp-gn	245	−2.0
			galena	−4.3	2.7(244± 38)	245	−2.0
	WS-7-1	Middle	chalcopyrite	0.2		230	0.4
Samchang	SC-10-2	Middle	pyrite	2.6	py-gn	215	0.9
			galena	−1.7	4.3(214± 30)	215	0.9
	SC-14	Late	sphalerite	−1.1	sp-gn	190	−1.6
			galena	3.6	2.5(264± 40)	190	−0.7
	SC-17	Middle	galena	−3.3		230	−0.8

[1] Data in parenthesis are sulfur isotope temperatures calculated using sulfur isotope fractionation equations compiled by Ohmoto and Rye (1979). [2] Based on fluid inclusion and/or sulfur isotope temperatures. [3] Calculated using sulfur isotope fractionation equations compiled by Ohmoto and Rye (1979).

and Epstein (1962), Hall and Friedman (1963), and Rye (1966). Data are reported in standard δ notation relative to the CDT standard for sulfur, the PDB standard for carbon, and SMOW standard for oxygen and hydrogen. The standard error of each analysis is approximately ± 0.1 per mil for sulfur, carbon, and oxygen, and ± 2 per mil for hydrogen.

Sulfur Isotope Study

Stage I sulfide minerals have $\delta^{34}S$ values that range from −4.3 to 2.6 per mil (Table 4). No systematic spatial or temporal variation of the $\delta^{34}S$ values of sulfides is observed.

The $\Delta^{34}S$ values of four mineral pairs yielded apparent equilibrium isotope temperatures between 214°± 30°C and 342°± 78°C (for Early Substage, 342° ± 78°C; for Middle Substage, 214°± 30°C and 244° ± 38°C; for Late Substage, 264°± 40°C) (Table 4). Apart from for the Late Substage, these sulfur isotope temperatures are in good agreement with the homogenization temperatures of primary fluid inclusions in associated minerals (Fig. 4). A temperature range of 214° to 244°C for pyrite-sphalerite-galena-electrum-argentite mineralization (Middle Substage) agrees well with the temperature range (230°± 15°C) determined from fluid inclusions in sphalerite (see "FLUID INCLUSION STUDIES").

Based on the fluid inclusion and/or sulfur isotope temperatures, $\delta^{34}S$ values of H_2S in stage I fluids were calculated (using the compiled data of Ohmoto and Rye, 1979). Calculated ranges of $\delta^{34}S_{H_2S}$ values based on the $\delta^{34}S$ values of sulfides are (Table 4): Early Substage sulfides, −0.9 to 0.8 per mil; Middle Substage sulfides, −2.0 to 0.9 per mil; and Late Substage sulfides, −1.6 to 0.3 per mil.

The calculated $\delta^{34}S_{H_2S}$ values for the hydrothermal fluids of the Weolseong and Samchang mines show small variations over a temperature range of 340° to 150°C. This may suggest dominance of H_2S in the fluids, because a temperature decrease of 190°C would have little effect on the $\delta^{34}S_{H_2S}$ value of a fluid if its sulfur were dominantly H_2S. Therefore, a maximum $\delta^{34}S_{H_2S}$ value of $\approx$ 1 per mil may be taken as an approximation of the sulfur isotope composition of the fluids ($\delta^{34}S_{\Sigma S}$).

However, we must also consider the probable presence of aqueous sulfates (e.g. SO_4^{2-}) in the fluids. Occurrences of hematite and barite in veins of the nearby Yonghwa and Suwang mines (Youn and Park, 1991; Park and Youn, 1991) may indicate a mixed H_2S-SO_4^{2-} character of the hydrothermal fluids in the Sulcheon area. Sulfate species in solution incorporate ^{34}S in preference to H_2S. Sulfur isotope fractionation between SO_4^{2-} and H_2S ranges from 20.0 to 35.4 per mil at temperatures between 150° and 340°C (Ohmoto and Rye, 1979). Therefore, the presence of sulfate species in solution can greatly affect the $\delta^{34}S_{\Sigma S}$ value.

A $\delta^{34}S_{\Sigma S}$ value of about 4 per mil was obtained for the epithermal system of a mine located approximately 25 km northeast of Sulcheon (the Wolyu Ag-Au mine whose mineralization dates at 79 Ma; Yun et al., 1992). Assuming that a $\delta^{34}S_{\Sigma S}$ value of 4 per mil represents the overall isotopic composition of magmatically-derived sulfur in Late Cre-

Table 5. Carbon, oxygen, and hydrogen isotope data for samples from the Weolseong and Samchang Au-Ag mines.

Mine	Sample no.	Description	$\delta^{13}C$(‰)	$\delta^{18}O$(‰)	T(°C)[1]	$\delta^{18}O_{water}$(‰)[2]	δD(‰)
Weolseong	WS-G-1	fresh granite (whole rock)		9.1			
	WS-G-2	sericitized granite (whole rock)		5.1			
	WS-G-3	ditto		4.2			
	WS-3-5	stage II vein calcite	−4.2	9.8	160	−2.1	
	WS-4-3	stage I vein quartz (middle)		3.7	245	−5.4	−74
	WS-5-1	ditto		4.3	235	−5.3	−70
Samchang	SC-10-2	stage I vein quartz (middle)		5.7	250	−3.2	−75

[1] Based on fluid inclusion temperatures. [2] Calculated using quartz-water and calcite-water oxygen isotope fractionation equations of Matsuhisa et al. (1979) and Friedman and O'Neil (1977), respectively.

taceous, gold-silver depositing fluids within the Youngdong-Muju mine district, we can calculate the H_2S/sulfate ratio of the fluid (using the $\Delta^{34}S$ values between SO_4^{2-} and H_2S, 20.0 to 35.4 per mil). If we assume an initial $\delta^{34}S_{\Sigma S}$ value of 4.0 per mil, so that the $\delta^{34}S$ values of H_2S during the mineralization at the Weolseong and Samchang mines are −2.0 to 0.9 per mil at 150° to 340°C, the probable H_2S/sulfate ratio of the fluid must have been about 8 : 2.

Carbon, Oxygen, and Hydrogen Isotope Study

The $\delta^{34}S$ value of one stage II calcite sample from the Weolseong mine is −4.2 per mil (Table 5).

The $\delta^{18}O$ values of three whole rock samples of porphyritic granite are: fresh granite, 9.1 per mil; and hydrothermally altered (sericitized) granite, 4.2 and 5.1 per mil (Table 5). The whole-rock $\delta^{18}O$ value of fresh granite (9.1 per mil) is similar with that of the Cretaceous Bulgugsa granites in South Korea (average 8.3 per mil; Kim et al., 1991). It is noteworthy that sericitized granites have much lower $\delta^{18}O$ values (at least 4 per mil lower) than the non-altered (fresh) granite. This indicates that the granite was isotopically depleted by interaction with isotopically lighter hydrothermal fluids ($\delta^{18}O$ of <4.2 per mil) (cf. Taylor, 1973, 1974) and therefore the hydrothermal fluids in the Sulcheon area were probably not related genetically with the intrusion of porphyritic granite.

The $\delta^{18}O$ values of three vein quartz samples from the Middle Substage of stage I range from 3.7 to 5.7 per mil (Table 5). Using the quartz-water oxygen isotope fractionation equation of Matsuhisa et al. (1979), coupled with primary fluid inclusion temperatures of each sample, the $\delta^{18}O$ values of waters in equilibrium with the stage I quartz are calculated to be −5.4 to −3.2 per mil. One stage II calcite sample has a $\delta^{18}O$ value of 9.8 per mil (Table 5), yielding a $\delta^{18}O_{water}$ value of −2.1 per mil, using the calcite-water oxygen isotope fractionation equation of Friedman and O'Neil (1977).

Fluids extracted from inclusions in 3 stage I vein quartz samples have δD values of −75 to −70 per mil (Table 5).

Interpretation of Oxygen and Hydrogen Isotope Data

Figure 8 shows the measured and calculated hydrothermal fluid compositions from the Weolseong and Samchang Au-Ag mines in the Sulcheon area (solid triangles) on a conventional hydrogen versus oxygen isotope diagram. These data are consistent with meteoric water dominance as fluid compositions approach those of local unexchanged meteoric waters.

Youn and Park (1991) reported a $\delta^{18}O$ value of 3.9 per mil for the alteration sericite from the nearby Yonghwa mine. Assuming a temperature of 340℃ for the sericite formation, a $\delta^{18}O_{water}$ value of 1.5 per mil can be calculated using the muscovite-H_2O oxygen isotope fractionation equation of Friedmen and O'Neil (1977). This $\delta^{18}O_{water}$ value is at least 3.6 per mil higher than our calculated data for vein fluids ($\delta^{18}O_{water}$ = −5.4 to −2.1 per mil). Assuming that the hydrothermal sericitic alteration mostly preceded the deposition of vein minerals (see "VEIN MINERALOGY"), we suggest that the oxygen isotope compositions of hydrothermal fluids decreased due to interaction with progressively larger volumes of meteoric water with time.

COMPARISON WITH OTHER KOREAN EPITHERMAL GOLD-SILVER DEPOSITS

Several epithermal gold-silver vein deposits in South Korea have been the subjects of recent

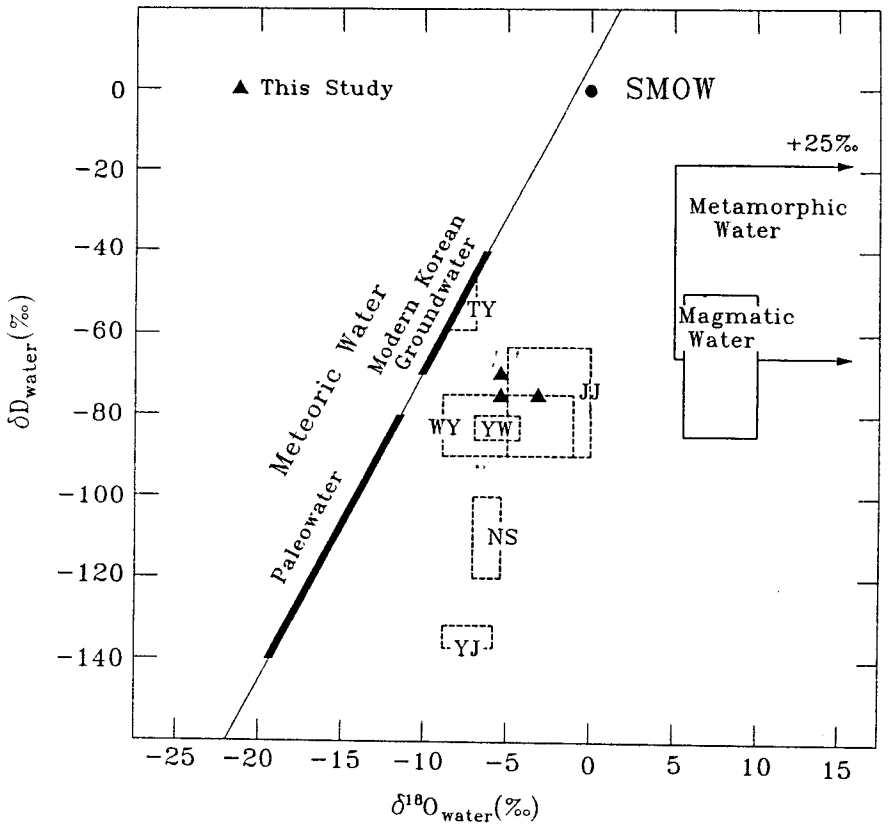

Fig. 8. Hydrogen versus oxygen isotope diagram, displaying stable isotope systematics of hydrothermal fluids from Late Cretaceous gold-silver deposits in South Korea. Solid triangles are values for Weolseong-Samchang. The magmatic and metamorphic water boxes (Taylor, 1974) and the meteoric water line (Craig, 1961) are shown. The ranges of δD values of paleometeoric (Mesozoic) waters and modern groundwaters in Korea are from Shelton et al. (1990) and Kim and Nakai (1988), respectively. Labeled boxes represent ore fluids from the following Korean Au-Ag deposits: JJ=Jeongju (So et al., 1991b): NS=Nonsan (So et al., 1987); TY=Tongyoung (Shelton et al., 1990); WY=Wolyu (Yun et al., 1992); YJ=Yeoju (So and Shelton, 1987); YW=Yangpyeong-Weonju (So et al., 1989).

geologic and geochemical studies (Table 6). They show several similarities, such as in Au/Ag ratios of ores, mineralogy, paragenesis, alteration assemblages, age, mineralization temperatures, ore fluid compositions, pressure-depth conditions, stable isotope compositions of ore fluids, and ore deposition mechanism(s). However, the geology of these deposits is rather diverse. For example, the Wolyu and Tongyoung deposits are hosted in Cretaceous, volcanic and sedimentary rocks.

Their ores have gold/silver ratios that range from 1.4:1 to 1:207, but they are typically silver-rich. Shelton et al. (1988) suggested that the gold/silver ratios of Korean vein-type gold-silver deposits relates directly to their depths of formation.

The Korean epithermal gold-silver deposits were formed by open-space filling along mostly N-S trending fault zones. Gangue minerals are mainly quartz with some rhodochrosite and calcite. Gold-silver commonly occur as electrum and argentite. Minor amounts of Ag-Sb(−As) sulfosalts and native silver are also present in the more silver-rich deposits. Various silver tellurides (hessite, stuetzite, empressite) and a Ag-Ge-S mineral (argyrodite) have been reported respectively in the volcanic and sedimentary rock-hosted, Tongyoung and Wolyu deposits. Hydrothermal wall-rock alteration characteristically consists of silicic and sericitic assemblages, with minor argillic assemblages. The pervasive presence of sericitic alteration in these deposits suggests that the pH of the ore fluids was nearly neutral (Hemley and Jones, 1964).

The ages of mineralization of these deposits fall in the narrow range from 90.5 to 67.5 Ma. Two main

Table 6. Comparison of features of some Late Cretaceous epithermal Au-Ag deposits in the Republic of Korea.

Mine or mine district	Geology	Au/Ag ratio	Vein			Alteration	Age of Mineralization(Ma)	Fluid inclusions	
			Strike	Gangue min.	Au-Ag min.			T(°C)[1]	Salinity(wt. % eq. NaCl)
Yeoju	Granite (156, 162 Ma) in gneiss	1 : 27~1 : 67	NS	qtz	el, arg	silicic, sericitic, argillic	88.2± 3.7	183 to 360 (185~285)	2.6 to 9.2
Nonsan	Quartz-feldspar porphyry and granite(Cretaceous ?) in metasedimentary rocks	1 : 207	NS	qtz, rhodo	el, arg, Ag-Sb(As)-S, ag	silicic, sericitic, minor argillic	71.1± 2.7	207~343 (225~285)	0.9 to 6.4
Yangpyeong-Weonju	Granite(79,104 Ma) in gneiss	1 : 1	NS~N10°W	qtz	el, arg	silicic, sericitic, minor argillic	67.5± 1.6	160 to 347 (180~260)	2.9 to 8.9
Tongyoung	Granodiorite (105 Ma) and volcanics	1 : 11	N50°-60°W	qtz, rhodo, cc	el, arg, Ag-Sb-S, Ag-tell, ag	silicic, sericitic, argillic	72.9± 1.2	146 to 282 (190~230)	1.0 to 6.1
Jeongju	Granite(140 Ma) in gneiss	1.4 : 1	NS~N20°W	qtz, cc	el, arg	silicic, sericitic, chloritic	74.8± 1.9	182 to 332 (180−270)	1.7 to 6.1
Wolyu	Quartz porphyry (82 Ma) in volcanosedimentary rocks	1 : 86	N5°-10°E	qtz, various carbonates	el, arg, Ag-Sb(As-Ge)-S, ag	silicic, sericitic, chloritic	78.9± 1.2	198 to 365 (200~280)	1.4 to 5.4
Weolseong-Samchang	Granite(102 Ma) in gneiss	1 : 5	N10°-25°W	qtz, cc	el, arg	silicic, sericitic, chloritic	90.5± 1.1	138 to 338 (190~270)	0.2 to 6.6

Mine or mine district	Fluid inclusions		Stable isotopes			Ore deposition mechanism(s)	Reference
	CO_2 contents	Depth(m)	$\delta^{34}S$(‰)[2]	$\delta^{18}O_{water}$(‰)	δD_{water}(‰)		
Yeoju	<0.5 mole %	500 to 1,250	0.9 to 9.5(≈ 8)	−8.8 to −4.2	−144 to −132	boiling and cooling	So and Shelton (1987)
Nonsan	<0.5 mole %	350 to 850	1.7 to 7.1(≈ 7)	−7.5 to −2.0	−120 to −100	meteoric water mixing after boiling	So et al. (1987)
Yangpyeong-Weonju	<0.4 mole %	220 to 550	−0.2 to 9.6(≈ 9)	−15.7 to −3.8	−111 to −81	meteoric water mixing after boiling	So et al. (1989)
Tongyoung	none	<1,000	3.6 to 8.2(≈ 5)	−9.4 to −6.7	−61 to −44	meteoric water mixing	Shelton et al. (1990)
Jeongju	<0.5 mole %	≈ 400	1.5 to 6.4(≈ 5)	−11.2 to +0.3	−109 to −65	meteoric water mixing after boiling	So et al. (1991 a, b)
Wolyu	none	370 to 600	3.2 to 7.3(≈ 4)	−8.7 to +3.8	−90 to −77	meteoric water mixing	Yun et al. (1992)
Weolseong-Samchang	none	400 to 700	−4.3 to 2.6(>1)	−5.4 to −2.1	−75 to −70	meteoric water mixing	This study

[1] Data in parenthesis refer to esimated Au-Ag deposition temperatures, [2] Number in parenthesis is an estimated $\delta^{34}S$ value of total sulfur in fluids
Abbreviations: ag=native silver, Ag-tell=silver tellurides, arg=argentite, cc=calcite, el=electrum, min.=minerals, qtz=quartz, rhodo=rhodochrosite.

granitic intrusive episodes are recognized in Korea: one in the Jurassic and one in the Cretaceous. The Jurassic granites are thought to have been intruded to depths of greater than 5 km, whereas the Cretaceous granites have been shown to be much shallower (<2~3 km) (Reedman et al., 1973; Tsusue et al., 1981). Epithermal gold-silver occurrences in Korea are all Late Cretaceous, and this indicates that they are associated with shallow, Cretaceous granitic activity.

Homogenization temperatures of fluid inclusions from Korean epithermal gold-silver deposits range widely from 138° to 365°C. Within this range, gold-silver deposition occurred at temperatures between 180° and 285°C (the higher temperatures within this range correspond to gold deposition, whereas lower temperatures correspond to the main silver deposition). Ore fluid salinities range from 0.2 to 9.2 wt. % eq. NaCl; and CO_2 contents of fluids (determined during crushing of fluid inclusions for hydrogen isotope analysis) are low (<0.5 mole %). Depths of mineralization are typically shallow (mostly less than 850 m).

Sulfur isotopic compositions ($\delta^{34}S$) of sulfides from Korean epithermal gold-silver deposits range from −4.3 to 9.6 per mil. The $\delta^{34}S_{\Sigma s}$ values of hydrothermal fluids have been estimated to be >1 (and ≈ 4) to ≈ 9 per mil. These $\delta^{34}S_{\Sigma s}$ values indicate that sulfur in ore fluids was largely derived from igneous sources. The higher (>7 per mil) $\delta^{34}S_{\Sigma s}$ values were obtained from some gneiss (probably paragneiss)-hosted deposits. Possibly, an isotopically lighter igneous source of sulfur (possibly ≈ 4 per mil) mixed with an isotopically heavier wall-rock sulfur (>9 per mil).

Oxygen and hydrogen isotope compositions of hydrothermal fluids were estimated as follows: $\delta^{18}O_{water} = -15.7$ to $+3.8$ per mil; and $\delta D_{water} = -144$ to -44 per mil. The stable isotope systematics of hydrothermal fluids from Korean epithermal gold-silver deposits are also shown in Figure 8. All the data display various degrees of ^{18}O enrichment relative to meteoric water, produced by exchange with hot igneous or wall rocks, the classic ^{18}O shift (Taylor, 1974). However, individual mines and districts have relatively narrow ranges of isotope conpositions. The wide range of δD values of hydrothermal fluids may represent large hydrogen isotope variations of paleometeoric water at the times of mineralization in these deposits, because most mineral-H_2O fractionation factors for hydrogen are negative, resulting in isotopically heavier water compositions due to water-rock interaction.

The ranges of all data (Fig. 8) are consistent with meteoric water dominance, and this is not surprising in the shallow (mostly <850 m) Au-Ag systems. It is interesting that the Tongyoung data fall on the meteoric water line, indicating that the Tongyoung Ag-Au system had the lowest degree of water-rock interaction, and probably occurred at the most shallow depths.

Precious-metal ore deposition in Korean epithermal gold-silver deposits was mainly a result of cooling of ore fluids by progressive mixing with cooler meteoric waters. Although boiling of hydrothermal fluids was reported in some deposits, fluid boiling probably occurred prior to the main gold-silver deposition, and therefore seems not to have been a genetically important mechanism of gold-silver depositions.

ACKNOWLEDGEMENTS

This paper was supported by Non Directed Research Fund, Korea Research Foundation, 1991. The authors thank the Center for Mineral Resources Research and Korea University for partial support of our field survey and isotopic analyses. We are grateful for constructive comments on the manuscript by Dr. M. J. Branney (Liverpool Univ., England).

REFERENCES

Barton, P.B. Jr. and Toulmin, P.III (1964) The electrum tarnish method for determination of the fugacity of sulfur in laboratory sulfide systems. Geochim. Cosmochim. Acta, v. 33, p. 841-857.

——— (1966) Phase relations involving sphalerite in the Fe-Zn-S system. Econ. Geol., v. 61, p. 804-826.

Choo, S.H. and Kim, S.J. (1985) A study of Rb-Sr age determinations on the Ryeongnam Massif (I): Pyeonghae, Buncheon and Kimcheon granite gneisses. Annual Report 85-24, Korea Inst, Energy and Resources, p. 7-38 (in Korean).

Craig, H. (1961) Isotopic variations in meteoric waters. Science, v. 133, p. 1702-1703.

Crawford, M.L. (1981) Phase equilibria in aqueous fluid inclusions. Mineralog. Assoc. Canada Short Course Handb., v. 6, p. 75-100.

Ellis, A.J. and Golding R.M. (1963) The stability of carbon dioxide above 100°C in water and sodium chloride solutions. Am. Jour. Sci., v. 261, p. 47-60.

Friedman, I. and O'Neil, J.R. (1977) Compilation of stable isotope fractionation factors of geochemical interest, *in* Fleischer, M., ed., Data of Geochemistry (6th ed.). U.S. Geol. Survey, Prof. Paper 440-KK, p. KK1-KK12.

Grinenko, V.A. (1962) Preparation of sulfur dioxide for isotopic analysis. Zeitschr. Neorgan, Khimii, v. 7, p. 2478-2483.

Haas, J.L. Jr. (1971) The effect of sanlinity on the maximum thermal gradient of a hydrothermal system at hydrostatic pressure. Econ. Geol., v. 66, p. 940-946.

Hall, W.E. and Friedman, I. (1963) Composition of fluid inclusions, Cave-in-Rock fluorite district, Illinois and Upper Mississippi Valley zinc-lead district. Econ. Geol., v. 58, p. 886-911.

Hedenquist, J.W. and Henley, R.W. (1985) The importance of CO_2 on freezing point measurements of fluid inclusions: Evidence from active geothermal systems and implications for epithermal ore deposition. Econ. Geol., v. 80, p. 1379-1406.

Helgeson, H.C. (1969) Thermodynamics of hydrothermal systems at elevated temperatures and pressures. Am. Jour. Sci., v. 267, p. 729-804.

Hemley, J.J. and Jones, W.R. (1964) Chemical aspects of hydrothermal alteration with emphasis on hydrogen metasomatism. Econ. Geol., v. 59, p. 538-569.

Kim, K.H., Lee, J.S., and Mizutani, Y. (1991) Petrogenetic studies of Mesozoic granites in South Korea. Abstracts of Geol. Soc. Korea Ann. Mtg., Seoul, 1991 (in Korean).

Kim, K.H. and Nakai, N. (1988) Isotopic compositions of precipitations and ground waters in South Korea. Jour. Geol. Soc. Korea, v. 24, p. 37-46 (in Korean).

Kim, O.J. (1975) Metallogenic epochs and provinces of South Korea. Jour. Geol. Soc. Korea, v. 7, p. 37-59.

Kretschmar, U. and Scott, S.D. (1976) Phase relations involving arsenopyrite in the system Fe-As-S and their application. Can. Mineralogist, v. 14, p. 364-386.

Lee, S.W. (1986) Metamorphism of the Gneiss Complex in the Southwestern Region of the Sobaegsan Massif: *in* Memoirs in Celebration of the Sixtieth Birthday of Professor Sang Man Lee, Seoul Natl. Univ., Seoul, p. 133-153 (in Korean).

Mann, H.B. and Whitney, D.R. (1947) On a test of whether one of two variables is stochastically larger than the other. Ann. Math. Statist., v. 18, p. 52-54.

Matsuhisa, Y., Goldsmith, R., and Clayton, R.N. (1979) Oxygen isotope fractionation in the system quartz-albite-anorthite-water. Geochim. Cosmochim. Acta, v. 43, p. 1131-1140.

McCrea, J.M. (1950) The isotope chemistry of carbonates and a paleotemperature scale. Jour. Chem. Physics, v. 18, p. 849-857.

Ohomoto, H. and Rye, R.O. (1979) Isotope of sulfur and carbon, *in* Barnes, H.L., ed., Geochemistry of hydrothermal ore deposits. New York, John Wiley Intersci., p. 509-567.

Park, H.I. and Youn, S.T. (1991) Gold and silver mineralization in the Suwang (Narim) mine(Abs.). Abstracts of Korean Inst. Mining Geol. Ann. Mtg., Pusan, 1991 (in Kerean).

Potter, R.W., II, Clynne, M.A., and Brown, D.L. (1978) Freezing point depression of aqueous sodium chloride solutions. Econ. Geol., v. 73, p. 284-285.

Reedman, A.J., Fletcher, C.J.N., Evans, R.B., Workman, D.R., Yoon, K.S., Rhyu, H.S., Jeong, S.H., and Park, J.N. (1973) Geological, geophysical and geochemical investigations in the Hwanggangri area, Chungcheong bug-do. Geol. Mining Inst. Korea Rept., Geol. Mineral Expl., v. 1, part 2, p. 1-119.

Robie, R.A., Hemingway, B.S., and Fisher, J.R. (1978) Thermodynamic properties of minerals and related substances at 298.15°K and one bar (10^5 Pascals) pressure and at higher temperatures. U.S. Geol. Survey Bull. 1452, 456p.

Roedder, E. (1984) Fluid inclusions. Rev. Mineralogy, v. 12, 644p.

Rye, R.O. (1966) The carbon, hydrogen, and oxygen isotopic compositions of the hydrothermal fluids responsible for the lead-zinc deposits at Providencia, Zacatecas, Mexico. Econ. Geol., v. 61, p. 1399-1427.

Seward, T.M. (1976) The stability of chloride complexes of silver in hydrothermal solutions up to 350°C. Geochim. Cosmochim. Acta, v. 37, p. 1329-1341.

——— (1984) The transport and deposition of gold in hydrothermal systems, *in* Foster, R.P., ed., Gold '82: The Geology, Geochemistry and Genesis of Gold Deposits. Geol. Soc. Zimbabwe Spec. Pub., v. 1, p. 165-181.

Shelton, K.L. and Orville, P.M. (1980) Formation of synthetic fluid inclusions in natural quartz. Am. Mineralogist, v. 65, p. 1233-1236.

Shelton, K.L., So, C.S., and Chang, J.S. (1988) Gold-rich mesothermal vein deposits of the Republic of Korea: Geochemical studies of the Jungwon gold area. Econ. Geol., v. 83, p. 1221-1237.

Shelton, K.L., So, C.S., Haeussler, G.T., Chi, S.J., and Lee, K.Y. (1990) Geochemical studies of the Tongyoung gold-silver deposits, Republic of Korea: Evidence of meteoric water dominance in a Te-bearing epithermal system. Econ. Geol., v. 85, p. 1114-1132.

Shimazaki, H., Sato, K., and Chon, H.T. (1981) Mineralization associate with Mesozoic felsic magmatism in Japan and Korea. Mining Geology, v. 31, p. 297-310.

Shimazaki, H., Lee, M.S., Tsusue, A., and Kaneda, H. (1986) Three epochs of gold mineralization in South Korea. Mining Geology, v. 36, p. 265-272.

Siegel, S. (1956) Nonparametric Statistics for the Behavioral Sciences: McGraw-Hill Inc., New York.

So, C.S. and Shelton, K.L. (1987) Fluid inclusion and stable isotope studies of gold-silver-bearing hydrothermal vein deposits, Yeoju mining district, Republic of Korea. Econ. Geol., v. 82, p. 1309-1318.

So, C.S., Chi, S.J., and Shelton, K.L. (1987) Stable isotope and fluid inclusion studies of gold-silver-bearing vein deposits, Cheonan-Cheongyang-Nonsan mining district, Republic of Korea. Nonsan area: Neues Jahrb. Mineralogie Abh., v. 158, p. 47-65.

So, C.S., Choi, S.H., Lee, K.Y., and Shelton, K.L. (1989) Geochemical studies of hydrothermal gold deposits, Republic of Korea: Yangpyeong-Weonju area. Jour. Korean Inst. Mining Geol., v. 22, p. 1-16.

So, C.S., Yun, S.T., Chi, S.J., Koh, Y.K., and Choi, S.H. (1991a) Cretaceous epithermal Au-Ag mineralization in

the Muju-Yeongam district (Jeongju mineralized area), Republic of Korea: Geologic, mineralogic, and fluid inclusion studies. Jour. Geol. Soc. Korea, v. 27, p. 451-470.

So, C.S., Yun, S.T., Choi, S.G., Koh, Y.K., and Chi, S.J. (1991b) Cretaceous epithermal Au-Ag mineralization in the Muju-Yeongam district (Jeongju mineralized area), Republic of Korea. Galena-lead and stable isotope studies: Jour. Geol. Soc. Korea, v. 27, p. 569-586.

Sourirajan, S. and Kennedy, G.C. (1962) The system H_2O-NaCl at elevated temperatures and pressures. Am. Jour. Sci., v. 260, p. 115-141.

Sterner, S.M. and Bodnar, R.J. (1984) Synthetic fluid inclusions in natural quartz I. Compositional types synthesized and applications to experimental geochemistry. Geochim. Cosmochim. Acta, v. 48, p. 2659-2668.

Taylor, H.P.Jr. (1973) $^{18}O/^{16}O$ evidence for meteoric-hydrothermal alteration and ore deposition in Tonophah, Comstock Lode, and Goldfield mining districts, Nevada. Econ. Geol., v. 68, p. 747-764.

——(1974) The application of oxygen and hydrogen isotope studies to problems of hydrothermal alteration and ore deposition. Econ. Geol., v. 69, p. 843-883.

Taylor, H.P.Jr. and Epstein, S. (1962) Relationship between $^{18}O/^{18}O$ ratios in coexisting minerals in igneous and metamorphic rocks-part 1. Principles and experimental results. Geol. soc. Am. Bull., v. 73, p. 461-480.

Tsusue, A., Mizuta, T., Watanabe, M., and Min, K.G. (1981) Jurassic and Cretaceous granitic rocks in South Kora. Mining Geology, v. 31, p. 260-280.

Youn, S.T. and Park, H.I. (1991) Gold and silver mineralization in the Yonghwa mine. Jour. Korean Inst. Mining Geol., v. 24, p. 107-129 (in Korean).

Yun, S.T., So, C.S., Choi, S.H., and Shelton, K.L. (1992) Genetic environment of germanium-bearing gold-silver vein ores from the Wolyu mine, Republic of Korea. Mineralium Deposita, v. 27 (in press)

Manuscript received 27 May 1992

韓半島 茂朱-靈岩지역 白堊紀 淺熱水 金-銀 鑛化作用 연구 (雪川지역 鑛化帶)

蘇七燮* · 尹聖澤** · 崔尙勳* · 金世鉉*** · 金炆榮****

요 약: 雪川지역 광화대내 月城 및 三倉광산의 淺熱水性 金-銀 脈狀 광화작용은 선캠브리아기 片麻岩類와 白堊紀(102 Ma) 斑狀 화강암 내에 발달하는 단층열극을 충진·배태한다. 광화작용은 구조적으로 크게 2회에 걸쳐 진행되었으며, 그 시기는 후기 白堊紀(90.5 Ma)이다. 流體包有物 및 광물학적 연구에 의하면, 광화 I기 중 석영-황화광물-에렉트럼-휘은석의 침전은 약 400~700 m의 淺深에서 0.2~6.6 wt. % NaCl 相當鹽濃度의 유체로부터 초기 약 340℃로부터 후기 약 140℃에 이르는 비교적 넓은 온도 범위에서 진행되었다. 流體-流體 혼합에 대한 통계학적 모델 평가에 의하면, 深部源 열수 유체와 淺部 순환 天水 사이의 혼합비는 광화작용의 진행과 더불어 점차 감소하였음을 지시한다. 금-은 광물의 침전은 순환 천수의 혼입에 따른 광화유체의 냉각 작용에 기인, 230°±40℃의 좁은 온도 범위에서 진행되었다.

산소 및 수소 安定同位元素 분석연구에 의하면, 광화 유체는 일차적으로 순환 천수로부터 기원하였고, 그 동위원소 조성은 동위원소적으로 진화하지 않은 순환천수의 값에 매우 근접하였음을 나타낸다.